# FEA OF CONVEYOR BELT SPLICE CORD END CONDITIONS

Greg WHEATLEY[1] and Soheil KEIPOUR[2]

*This analysis focuses on optimization techniques pertaining to the use of finite element software, and the fatigue component of the splice design.*

*Firstly, the focal point is on the replication of the adhesive behavior that the bonding displays between the steel cord and rubber. So, single cord and multi-cord models were developed and investigated to determine stress induced due to static pull-out force.*

*Secondly, three different cord ends were applied to a rubber belt section under static pull-out with a constant force to determine which end shape showed the lowest stress concentration. The cord with the square end was found to show the lowest stress concentration.*

**Keywords**: Conveyor, Belt Splice, Steel Cord, Rubber, FEA.

## 1. Introduction

The conveyor belt is a complicated component to engineer due to the hyper-elastic nature of rubbers, and the inherent composite nature of its structure. It has proven a difficult task in recent years to accurately simulate non-linear materials using FEA. Quality of workmanship during vulcanization is key to splice strength, along with physical dimensions of the layout. As the belts undergo repetitive cyclic fatigue, it is important to achieve maximum durability of the splice. This can be done through FEA optimization techniques to achieve the highest dynamic efficiency possible.

Belt conveyors are currently the cheapest, most effective, and efficient means of transportation of bulk materials [1, 2]. This high efficiency makes them valuable assets that are implemented in a multitude of industries ranging from mining, food and supplies, electrical power, manufacturing, metallurgy and chemical processes [3]. The splice is considered the weakest part of the conveyor belt, with approximately 93.75% of belt failure occurring in this location [1-7].

Cord diameter increase has an enormous effect on the overall strength of the conveyor belt [4]. It has been found that there is a proportional increase in the pull-out force with the increase in cord diameter [7]. Li, et al. found that cord pitch is extremely important in optimization of belt splices [1] and an increase in steel cords does increase pull-out force [4].

[1] Prof., Dept. of Mechanical Engineering, James Cook University, Australia, e-mail: greg.wheatley@jcu.edu.au

[2] Postgraduate, Shahrood University of Technology, Iran, e-mail: soheil.keipour@gmail.com

Finite element method (FEM), coupled with the superior processing capabilities of modern technology, is a vital tool in the design and fatigue assessment of conveyor belts [1, 5, 8, 9]. Current software and analysis methods are getting better at modelling the non-linear, hyper elastic behavior, with one such method using the Mooney-Rivlin model [1, 3-6]. Marasová modelled the conveyor belt resistance to puncture, and Bindzár modelled the static and dynamic stress of conveyor belt while applying the Finite Element Method [10, 11]. In 2011, Bai Chengcheng et al. analyzed the pull-out process of a single steel cord in the steel cord conveyor belt and the mechanical characteristics after the steel cord rupture by using finite element software and some achievements have been obtained. However, the research only stayed on a single steel cord modeling analysis, no further analysis of the tows of multiple steel cords, and no numerical simulations validated by experimental result [12]. Chen Lin et al. proposed a finite element analysis method of dynamic fatigue of a single steel cord of a steel cord conveyor belt and shows that the main damage location of the steel cord conveyor belt in the bonding area of the steel cord and the rubber [13]. Du Wenzheng et al. found a method of steel cord stress analysis and a study of fatigue life. Finite element analysis shows that the stress of the steel cord is distributed spirally in space, and the Von-Mises equivalent stress at the contact between the core cord and the inner steel cord is the maximum and the fatigue life is the minimum [14].

Repetitive FEA simulation coupled with experimental testing is the best method for optimizing conveyor belt mechanical properties. However, inconsistencies in manufacturing and preparation of belts, as well as discontinuities in the material, pose the greatest source of belt failure [8]. In order to achieve the best possible result, correct splicing procedures must be maintained at all times, otherwise optimization techniques become redundant.

## 2. Design development and analysis

### 2.1 Design development

Manufacturers follow the standards in construction of the belts, where the main differences are generally minor changes in cover thicknesses, cord diameters, and insulation rubber. The focus of this experiment is in optimizing this design, and subtle changes in areas of high stress concentration that could potentially improve strength or fatigue life while minimizing material usage. As such, the initial design focused on the use of a St-1000 (The ‘St’ component denotes the type being a steel cord belt, whilst the number on the end represents the force rating in kN/mm belt width) belt for development of the model, and all dimensions were based off the specifications from one manufacturer. The layout consists of a simple one step splice, thus reducing complexity of the initial

analysis, where any efficiency increases could be potentially paralleled to larger belts in subsequent analyses.

The preliminary load case focused on a simple design consisting of a single steel cord embedded in the rubber carcass, with a static pull-out force applied to one end. For a St-1000 conveyor belt, the standard operating tension is around 140 N/mm, and the pull-out force is approximately 80 N/mm. For static tests, DIN22102 [15] requires a reference tension of 10% of the belt's nominal breaking strength. Using the specifications from the METSO manufacturer's brochure, the standard operating tension over an assumed 800 mm of belt width. The results were obtained and put in Table 1.

*Table 1*

**St-1000 conveyor belt operations**

| | $F_T$ (kN) | $F_B$ (kN) | $F_S$ (kN) | $F_C$ (kN) | Number of cords | Belt Stress $\sigma_B$ (MPa) | Individiual Cord Stress $\sigma_T$ (MPa) |
|---|---|---|---|---|---|---|---|
| Standard Operation | 64 | 112 | 32 | 1.016 | 63 | 0.345 | 0.095 |
| Maximum Tension | 480 | 800 | 240 | 7.62 | 63 | 2.464 | 0.709 |

Where, $F_B$ is the tension force in the belt and $F_T$ is the tension force in cord. $F_S$ denotes shear force between the cord and belt. $T_B$ is torsion generated due to movement and twist in the cord.

The second load case is the dynamic mode, where the belt is fatigued due to continuous operation and cyclic stress conditions. For fatigue testing of belt splices, DIN22131 [16] and AS1333 [17] recommend the range of the cyclic force be between around 3.6 – 36% of the nominal static pull-out strength for the given cord diameter. The minimum required dynamic efficiency and other conditions can be calculated using relevant standards.

## 3. ANSYS finite element analysis (FEA)

ANSYS has many built in hyper-elastic options such as the Mooney-Rivlin, Yeoh, Ogden, and Neo-Hookean models. These were each implemented independently to ensure conformity of results and allow comparison of data.

In order to simplify the design and decrease the node count in ANSYS, the rubber belt has been constructed as a rectangle, with the steel cord being extruded as a straight cylindrical boss (Figure 3). It is evident that the belt structure is A-symmetrical, thus the modelled belt can be cut in half to reduce the node count further, and increase the mesh detail around critical stress concentrations.

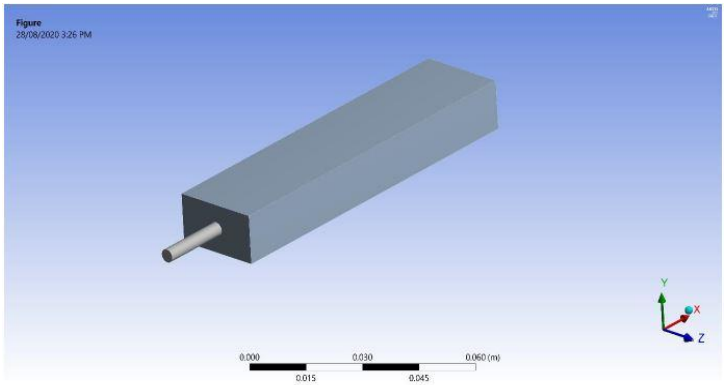


Fig. 3. Conveyor belt internal forces

This report will focus on a smaller belt to ensure that the material properties, characteristics, force and contact interactions are defined appropriately. Figure (4a) shows belt cross sectional dimensions. The belt behavior is established first based on a St-1000 belt from the provided manufacturer's belt guide (Table 2).

*Table 2*

**Manufacturer's belt guide**

| | Operating tension (N/mm) | Cord Dia. standard (mm) | Cord Dia. max. (mm) | Cord strength, min. (kN) | Cord pitch (mm) | Min. cover thickness (mm) | Belt weight, min. covers ($kg/m^2$) |
|---|---|---|---|---|---|---|---|
| St 1000 | 140 | 3.7 | 4.0 | 13.2 | 12.0 | 5/5 | 21.6 |

The steel cord is established as a linear-elastic steel to mimic the elasticity of wire ropes. As the properties and dimensions were readily available, the St-1000 was used (Table 3). Standard wire rope for steel cord conveyor belts is constructed as a series of intertwined galvanized wires as seen in Figure 4b. For the purposes of the initial testing and simulation, this geometry can be simplified to an extruded cylindrical body. For a belt of St-1000 specification, the standard diameter is around 3.7 – 4.0 mm.

*Table 3*

**Steel cord properties [1]**

| Property | Value |
|---|---|
| Density | 7850 $kg/mm^3$ |
| Poisson's Ratio | 0.28-0.29 |
| Modulus of Elasticity | 210 GPa |

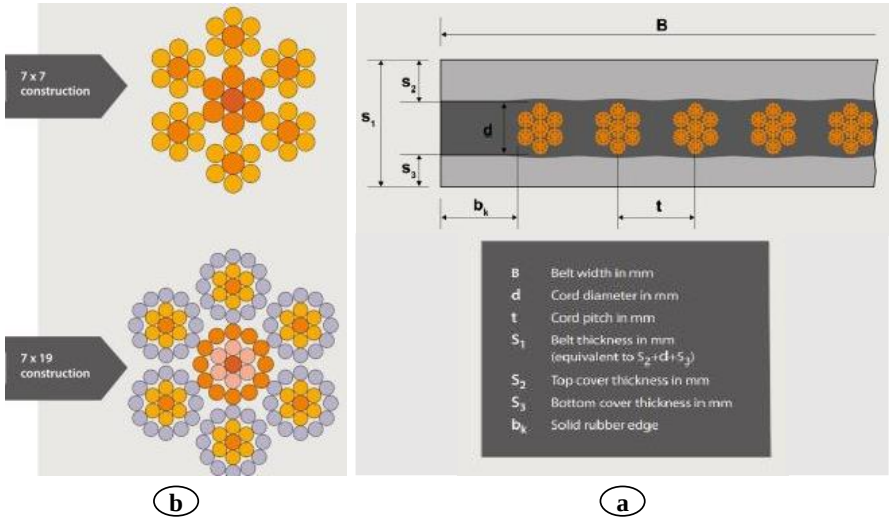


Fig. 4. a) Belt cross sectional dimensions, b) Steel cord wire construction

Rubber and other highly elastic materials lack homogeneity in terms of their physical properties and compositions. The properties utilized for the conveyor belt rubber were of a non-linear, hyper-elastic rubber. Several of the more common material models will be implemented to validate data and simulation results.

There are two methods to which the tension can be applied to the cord, via displacement, or a vector force. Both of these methods are viable options, although since a static force had been calculated in the load case scenario, the vector force application was selected. This was achieved numerically by implementing fixed supports on the sides and back of the belt module, with the vector force applied to the face of the singular steel cord.

It is a complex composite of linear elastic steel and hyper elastic rubber, which is bonded together in a pseudo adhesive manner. The most appropriate contacts in ANSYS for the specified application were determined to be Bonded Contact, Rough Contact and Frictional Contact.

From the contacts available, the frictional contact displays the most potential as a solution to the complex bonding at the interface. It allows sliding of the cord but also provides the shear stress resistance known as ‘sticking’. This is similar in nature to the adhesive bond of the vulcanized belt components. It is possible to input values for the coefficient of friction in ANSYS greater than 1. A value of 1 suggests that the frictional force is equal to the normal force, where a value greater than this simply means that the frictional force is stronger than the normal force. This could potentially be tuned by continually increasing the frictional coefficient until the simulated pull-out force approaches the experimental results.

### 3.1 Single cord pull-out tests

In the initial investigation, single cord pull-out was analyzed in order to determine the appropriate simulation configurations. This is covered in this report to show disparity between the different contact methods, and agreeance between alternate elastomer material models. The bonded (no separation), frictional (μ=2,000,000) and rough (infinitive friction) contacts were used under the Neo-Hookean, Yeoh and Mooney-Rivlin material models.

The bonded and rough contact were implemented with the cord also fixed at the opposite end to the applied force. This will not allow determination of the moment of failure of the cord bond, but will provide the maximum stress, strain and deformation for the given static loading application. The frictional contact focuses on utilization of the frictional coefficient between the rubber and steel cord as the support.

### 3.2 Multi-cord Pull-out tests

A new section of belt was designed for multi-cord testing (figure 6). Most of the settings were kept the same, with the only difference being that the forces are distributed across the belt. As the rough contact was determined to not replicate the behavior properly, and the hyper elastic materials provided consistent results, only the bonded and frictional contacts were used under the Mooney-Rivlin material model.

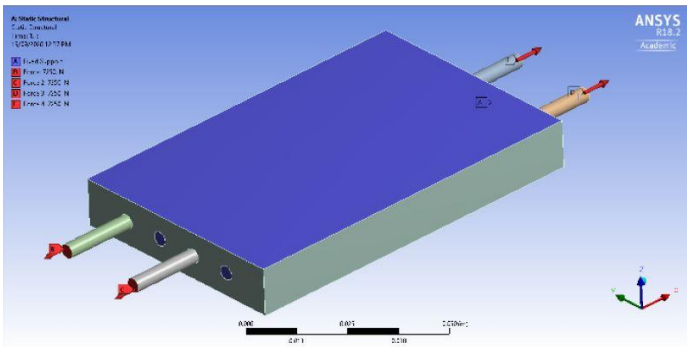


Fig. 6. Multi-cord model setup

### 3.3 Cord end investigation

The steel cord end is widely known to be the location of greatest stress concentration in the belt, and generally the area that causes failure. Due to this, it was decided that the interaction between the rubber and steel cord end was a focal point of the analysis. This investigation will utilize three different cord end variations, to determine which shape displays the maximum stress concentration.

Three different cord ends were trialled square, spherical, and chamfered. The actual values of the stress are unimportant, as the analysis purely aims to determine which cord end shows the greatest stress concentration. Due to this, the main requirement is that the contact method remains the same between the tests, as this will still show which has higher stress. The frictional contact is the preferred method from the previous analyses conducted, although the bonded contact was implemented due to simplicity of its setup, and will still show the disparity between the cord ends. Deformation, stress, and strain were all recorded for this analysis, but only the stress concentration at the end is of importance. The maximum force calculated from the static load case of $F_C$=7.62 kN was applied to the end of the cord in each case.

## 4. Results and discussion

### 4.1 Tensile test results

The figure 7 shows the engineering stress and strain plot.

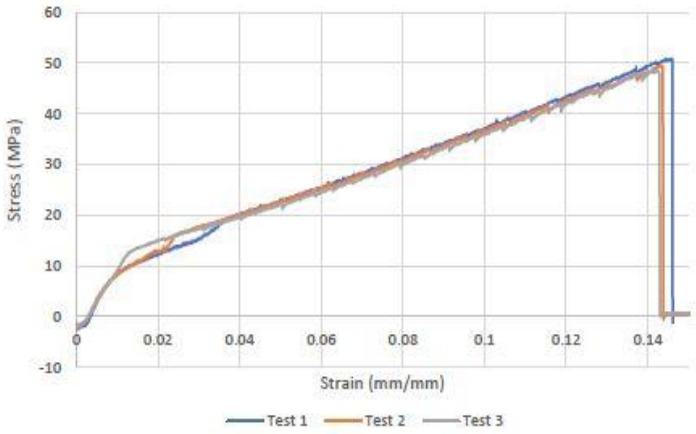


Fig. 7. Engineering stress and strain

Thus, from the analysis conducted the average stress and strain values at failure were calculated below in Table 4.

*Table 4*

**Average forces at failure**

| Parameter | Test 1 | Test 2 | Test 3 | Average |
|---|---|---|---|---|
| Displacement (mm) | 29.15 | 28.70 | 28.25 | 28.70 |
| Tensile Force (N) | 4324.68 | 4204.24 | 4136.67 | 4221.90 |
| Engineering Stress (MPa) | 50.88 | 49.46 | 48.67 | 49.67 |
| Engineering Strain | 0.14 | 0.14 | 0.14 | 0.14 |

### 4.2 Single cord pull-out results

Concluding the single cord pull-out analysis, the FEA results show reasonable agreement across the multiple hyper-elastic material models implemented, and the different contact methods used. Figure 8 and figure 9 show stress and deformation of model respectively. The available contacts applied to the model, the bonded and frictional contacts seem to replicate the interaction most accurately. Thus, these two contacts will be used moving forward, and the rough contact will be disregarded. The hyper-elastic material models all performed favorably, and there was good agreeance between the simulations. To limit the number of tests conducted, and also because researched literature suggests so, the Mooney-Rivlin model was used primarily for the remaining tests.

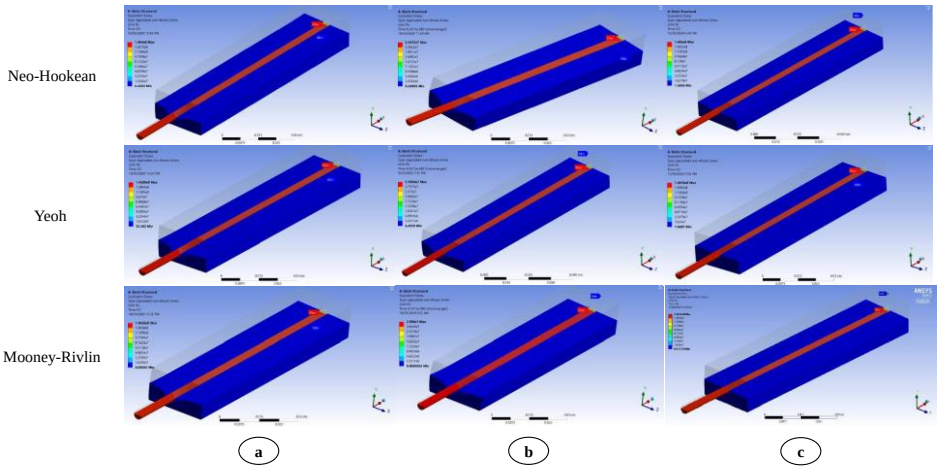


Fig. 8. Single cord stress, a) Bonded contact, b) Frictional contact and c) Rough contact

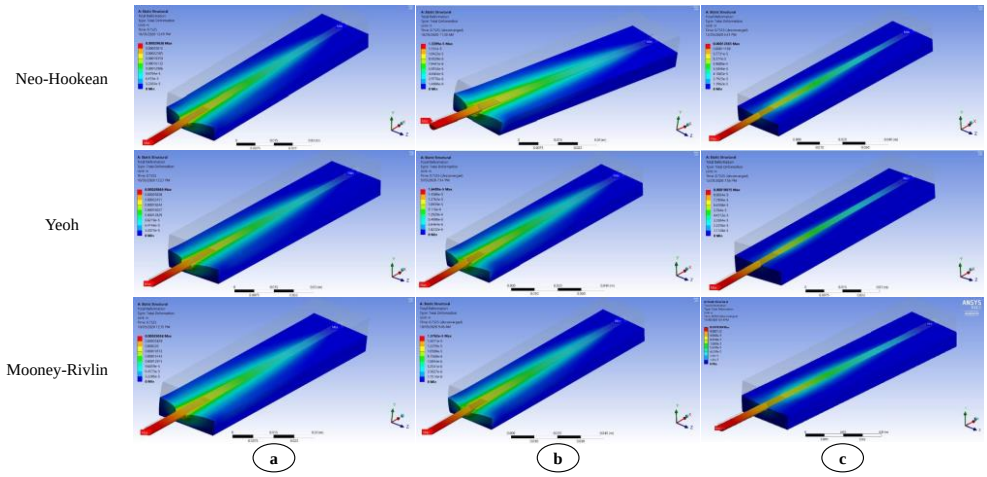


Fig. 9. Single cord deformation, a) Bonded contact, b) Frictional contact and c) Rough contact

Maximum deformation, stress, and strain from the analyses are quantified below in Table 5. As shown, the results of the bonded and rough contacts are rather similar, while the frictional model displays much lower stresses. It would be assumed as stated that the frictional contact is much closer to the actual replication of the interaction between the steel cord and rubber in comparison to the other contacts.

*Table 5*

**Single cord pull-out results**

| Contact Type | Hyper Elastic Model | Maximum Deformation (mm) | Maximum Strain (mm/mm) | Maximum Stress (MPa) |
|---|---|---|---|---|
| Bonded | Neo-Hookean | 0.00029038 | 0.045052 | 146.4 |
| | Yeoh | 0.00028866 | 0.042245 | 145.09 |
| | Mooney-Rivlin | 0.00029058 | 0.045055 | 146.56 |
| Frictional | Neo-Hookean | 0.000013399 | 0.0028176 | 25.473 |
| | Yeoh | 0.000016409 | 0.0033819 | 31.02 |
| | Mooney-Rivlin | 0.000015762 | 0.0033274 | 29.98 |
| Rough | Neo-Hookean | 0.00012565 | 0.015799 | 146.5 |
| | Yeoh | 0.00010015 | 0.0064049 | 146.16 |
| | Mooney-Rivlin | 0.0001269 | 0.016118 | 146.56 |

### 4.3 Multi-cord pull-out results

The multi-cord FEA results are quantified in figure 10 below.

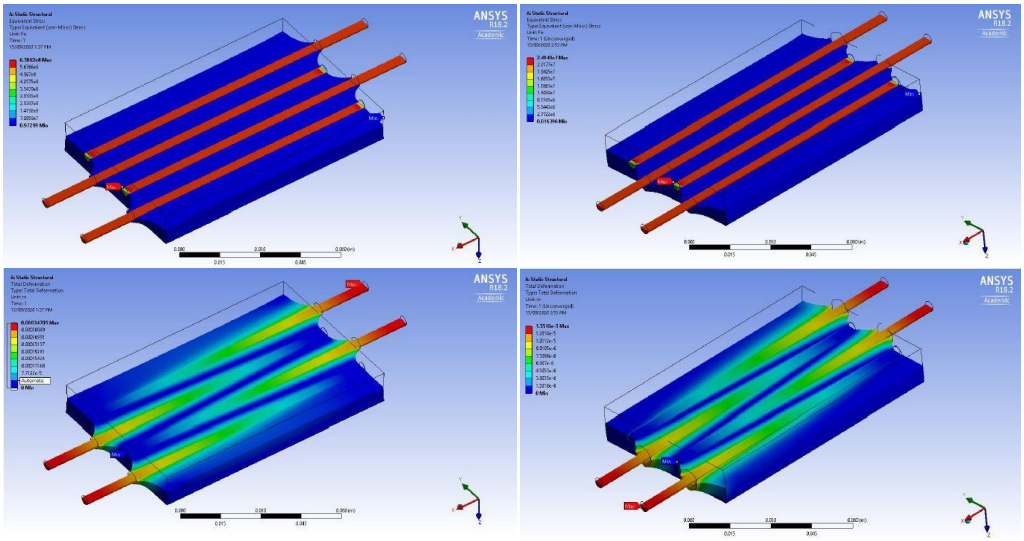


Fig. 10. a) Multi-cord Mooney-Rivlin stress (up) and deformation (down), a) Bonded contact, b) Frictional contact

As with the single cord analysis, the frictional contact has again produced the most reasonable results (Table 6).Where the maximum stress from the bonded contact was found to be 638.62 MPa, and that of the frictional contact was found to be 24.95 MPa. In further analyses, if the scope of the project is limited to the use of ANSYS, it would therefore be recommended to use the frictional contact.

*Table 6*

**Multi-cord pull-out results**

| Contact Type | Hyper Elastic Model | Maximum Deformation (mm) | Maximum Strain | Maximum Stress (MPa) |
|---|---|---|---|---|
| Bonded | Mooney-Rivlin | 0.00034705 | 0.068739 | 638.62 |
| Frictional | Mooney-Rivlin | 0.000013516 | 0.0020508 | 24.95 |

### 4.4 Cord end Results

From the ANSYS static belt tests conducted for varied cord end shape (figure 11), the results were obtained and put in Table 7 below.

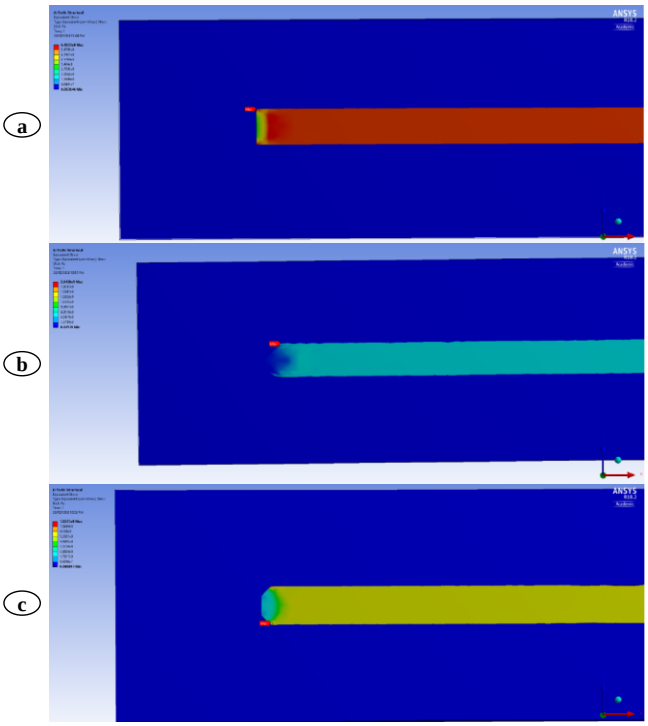


Fig. 11. Side views, a) square cord end, b) spherical cord end, c) chamfered cord end

*Table 7*

**Cord end shape maximum stress values**

| Cord end shape | Maximum Stress (MPa) |
|---|---|
| Square | 616.33 |
| Spherical | 2043.8 |
| Chamfered | 792.77 |

Using a bonded contact between the steel cord and rubber, with a maximum force of around 7000 N, it was found that the square end cord actually showed the lowest maximum stress at the cord end. However, more testing would be recommended before a conclusion can be made, such as implementing a contact that more appropriately replicates the adhesive bonding of the steel cord and rubber. This could potentially change the outcome of the investigation. The values of the stress shown are not representative of what might actually be found due to the contact method used, but still show that the lowest stress concentration is in that of the square end, followed by the chamfered end, and finally the spherical end.

## 6. Conclusions

A static pull-out test was conducted for single and multi-cord splice assemblies for varied contacts and hyper elastic material models for comparison. The standard hyper elastic material models defined by ANSYS are able to be applied and all maintained consistent results. The contacts in ANSYS are not appropriate for replication of the interaction between the steel cord and rubber, but still allow for the locations of maximum stress to be defined. The contact closest to replicating the conditions of the interaction between the steel cord and rubber was found to be the frictional contact. Maximum stress concentration from the FEA was found at the ends of the cord, as established previously in literature. An FEA analysis of three different cord end conditions suggested that the square end produced the lowest stress concentration of the options.

## R E F E R E N C E S

[1]. *X.Li, X.Long, H.Jiang and H.Long*,"Influence of different cord pitch on the pullout force of steel cord conveyor belt splice", in Journal of Adhesion Science and Technology, **vol. 32**, no. 20, Oct. 2018, pp. 2268-2281

[2]. *X.Long, X.Li and H.Long*,"Analysis of influence of multiple steel cords on splice strength", in Journal of Adhesion Science and Technology, **vol. 32**, no. 24, Dec. 2018, pp. 2753-2763

[3]. *W.Song, W.Shang and X.Li*,"Finite element analysis of steel cord conveyor belt splice", in International Technology and Innovation Conference, China, 2009

[4]. *X.Li, X.Long, Z.Shen and C.Miao*,"Analysis of Strength Factors of Steel Cord Conveyor Belt Splices Based on the FEM", in Advances in Materials Science and Engineering, **vol. 2**, Dec. 2019, pp. 1-9

[5]. *L.Nordell, X.Qiu and V.Sethi*,"Belt conveyor steel cord splice analysis using finite element methods", Bulk Solids Handling, **vol. 11**, no. 4, Nov. 1991, pp. 863-868

[6]. *X.Li, Y.Long, Q.Jiang and H.Long*,"Finite element simulation and experimental verification of steel cord extraction of steel cord conveyor belt splice", in IOP Conference Series: Materials Science and Engineering, **vol. 369**, no. 1, May. 2018, pp. 012025

[7]. *X.Long, X.Li, M.Sun and Z.Shen*,"Quantitative analysis of bond and splice strength of steel cord conveyor belt", in Journal of Adhesion Science and Technology, **vol. 34**, no. 14, Jan. 2020, pp. 1544-1555

[8]. *A.Harrison*,"Limitations of theoretical splice design for steel cord belts", in Bulk Solids Handling, **vol. 14**, no. 1, 1994, pp. 39-43

[9]. *A.Adams*,"FEA of steel cable conveyer belt splices", in Rubber World, **vol. 209**, Nov. 1993, pp. 32-32

[10]. D.*Marasová, M.Maras*,"Mathematical modelling of resistance of conveyor belts against puncture", T Tech Univ Košice, **vol. 4**, 1998, pp. 22–32

[11]. *P.Bindzár*,"Conveyor belt modelling by finite element method", Transport. Logist Int J., **vol. 6,** 2006, pp. 5

[12]. *C.Bai*,"Simulation and finite element analysis of the steel-cord conveyer belt on fragmentation", Shanghai: East China University of Science and Technology, 2011, pp. 16-18

[13]. L.*Chen, P.Ma, C.Wang, et al.*,"Finite element analysis of dynamic fatigue of a new steel cord conveyor belt (HHE) single steel wire", Chin Rubber, **vol. 12**, 2014, pp. 46–48

[14]. *W.Du, B.Ma, D.Cao, et al.*,"Research on stress and fatigue life of steel wire rope", Coal Eng., **vol. 49**, 2017, pp. 134–137.

[15]. DIN 22102 cz.3, German Industrial Standard, Textil- Fordergurte fur Schuttguter- Nich losbare Gurtverbindungen. In-stalling and Splicing Textile Conveyor Belts, ContiTech Conveyor Belt Group, 1991

[16]. DIN 22131, German Industrial Standard, Steel cord conveyor belts for general conveying: dimensions, requirements, 1988

[17]. AS 1333, Standards Australia, Conveyor belting of elastomeric and steel cord construction, 1994